Dynamics of contact radical ion pairs C_{60}—aromatic amines. A study by picosecond laser photolysis

*N. A. Nadtochenko,** *N. N. Denisov, and P. P. Levin*

Institute of Chemical Physics in Chernogolovka, Russian Academy of Sciences,
142432 Chernogolovka, Moscow Region, Russian Federation.
Fax: +7 (096) 515 3588

Charge transfer complexes between C_{60} and ternary aromatic amines (*N,N,N',N'*-tetramethyl-*p*-phenylenediamine, *p*-methoxy-*N,N*-dimethylaniline, *p*-methyl-*N,N*-dimethylaniline, *N,N*-diethylaniline, *N,N*-dimethylaniline, and triphenylamine) were studied in chlorobenzene solutions. The lifetimes of the excited state with charge transfer in these complexes were measured by the method of picosecond laser photolysis. The dependence of the rate constant of the back electron transfer on ΔG in the back electron transfer reaction with relaxation of the charge-transfer state exhibits the "Marcus-inverted" region.

Key words: contact radical ion pairs, aromatic amines, picosecond laser photolysis.

According to modern concepts, the rate constant of electron transfer k_{ET}, which determines the rate of charge separation in a redox reaction and charge recombination in radical ion pairs (RIPs), depends on several factors: (1) parameter of the electron-electron interaction (V); (2) free energy of the electron transfer reaction (ΔG); (3) reorganization energy (λ), which consists of two components: internal (λ_i) and external (λ_0) reorganization energies; (4) dynamic properties of the polar surroundings of the medium, which can be expressed by the longitudinal relaxation time of a dielectric (τ_L) related to the Debye relaxation time *via* the known expression: $\tau_L = (\varepsilon_o/\varepsilon_s)\tau_D$, where $\varepsilon_{o,s}$ are the optical and static dielectric permeabilities, respectively.[1–10] Studies of the electron transfer reactions in the recombination of charges photogenerated in the photoredox reaction are of special interest, because the situation in which the free energy ΔG is varied in a wide range in a series of reactions of the same type can be easily realized experimentally. The normal and/or "inverted" regimes of the electron transfer reaction depending on the value of ΔG have been observed in several works.[11–19] It is noteworthy that the normal and "inverted" regimes were observed simultaneously in the same series only for solvate-separated RIPs, *i.e.*, the pairs that are formed due to the quenching of excited (singlet or triplet) states by an electron donor or acceptor.[3,9,10,11,15] No normal regime was observed in the case of such contact RIPs as the photoexcited state with the charge transfer in the donor-acceptor complex D^+/A^-. The problem about the dependence of the electron transfer rate constant k_{ET} on ΔG for the back electron transfer in D^+/A^- in the charge-transfer complex (CTC) is vividly discussed in the literature.[11–21] It should be taken into account that the shapes of the absorption band and the fluorescence band with charge transfer in the CTC[2,7–9] are determined by the same Frank—Condon factor as the Frank—Condon factor that determines the rate constant of electron transfer.[1–9] This parallelism between the optical transition and electron transfer means that the plot of k_{ET} *vs.* ΔG should be similar to the shape of the band with the electron transfer. The fact that no "parabolic" dependence of the charge transfer rate constant k_{ET} on ΔG was observed for contact RIPs in the case of the CTC should be additionally studied.

Fullerene C_{60} has pronounced electron-withdrawing properties[22–24] and can form donor-acceptor complexes with molecules which possess electron-donating properties, for example, tertiary aromatic amines (Am).[25–29] In addition to this, it is reasonable to expect that the photoexcited singlet and triplet states of C_{60} are quenched by amines *via* an electron transfer mechanism to form radical ions in polar solvents and radical ion pairs (exiplexes) in the solvents of lower polarity. The formation of radical ions in the quenching of triplet-excited C_{60} by amines has previously been observed.[22,30,31] Charge-transfer complex formation between C_{60} and amines seems to be a convenient set of reactions for experimental study of electron transfer in contact RIPs, because the ΔG value is varied within 1 eV for the series of *N,N*-tetramethyl-*p*-phenylenediamine (TMPD), *p*-methoxy-*N,N*-dimethylaniline (MeODMA), *p*-methyl-*N,N*-dimethylaniline (MeDMA), *N,N*-diethylaniline (DEA), *N,N*-dimethylaniline (DMA), and triphenylamine (TPA). The purpose of this work is to study the electron transfer reactions in the contact RIPs of C_{60}

Translated from *Izvestiya Akademii Nauk. Seriya Khimicheskaya,* No. 6, pp. 1078—1089, June, 1995.

and Am in chlorobenzene by picosecond laser photolysis and the absorption spectra of CTC between C_{60} and Am in the series of tertiary aromatic amines and to analyze the parallelism between optical transitions and electron transfer in the series of these CTC.

Experimental

Chromatographically pure C_{60} synthesized by the known procedure[32] was used; the content of fullerene exceeded 98 %. Aromatic amines were purified by sublimation *in vacuo*, vacuum distillation in argon, or recrystallization from ethanol. Solvents were purified by standard procedures.

Absorption spectra of solutions were recorded on a Specord M-40 spectrophotometer. A HIPAD Plus standard digitizer was used for the formation of an absorption spectrum as an array of numerical data. Further numerical processing of absorption spectra was carried out using standard software packages for a personal computer. Equilibrium constants of the formation of CTC between C_{60} and Am were determined from the concentration dependence of the corresponding amine on the optical density of the solution of C_{60}, using the Benesi—Hildebrand procedure.[33]

Table 1. Spectral and energy parameters of the C_{60}—aromatic amine system

Amine	ΔG /eV	ν_{max} /cm^{-1}	$W_{1/2}$ /cm^{-1}	ϵ /M cm^{-1}	K /M^{-1}
TMPD	0.73	13750	6700	2200	0.44±0.03
MeODMA	1.16	16390	5150	2250	0.29±0.04
MeDMA	1.32	17800	5600	1750	0.61±0.04
DEA	1.37	17300	5300	2000	0.29±0.05
DMA	1.42	18450	5300	1700	0.45±0.02
TPA	1.73	17800	5100	2000	0.35±0.05

Note: ΔG is calculated from the electrochemical data; ν_{max} is the absorption band maximum; $W_{1/2}$ is the half-width of the charge-transfer band; ϵ is the extinction coefficient at the band maximum; K is the equilibrium constant.

The absorption spectra and decay kinetics of intermediate products in picosecond photolysis experiments were recorded by two laser photolysis installations: an installation based on an Nd^{3+}-aluminate laser with active-passive mode synchronization and an installation based on an Nd^{3+}-glass laser with passive mode synchronization. The experimental installation has been described in detail in Ref. 34. The duration of the generation pulse of the Nd-aluminate laser was 20 ps and 6 ps for the Nd-glass laser. The Nd-glass laser was used for recording fast relaxation processes in the systems with TMPD and MeODMA. The absorption spectra of intermediate products were obtained with the Nd-aluminate laser. Samples were excited by the second laser harmonics. In picosecond photolysis experiments, absorption spectra of intermediate states were obtained using the light of the picosecond continuum generated from the first harmonics in an $H_2O : D_2O$ mixture (50 : 50). The induced optical absorption was recorded by two photodiodes mounted behind a monochromator. The available spectral range of detecting was 430 to 1200 nm. Low excitation energies (no more than 1 mJ at the 2-mm aperture of the laser beam) were used to prevent undesirable processes of multi-photon ionization of amine molecules. The program for the solution of the inverse problem of extracting the signal from the observed signal convolution with the spread function (developed by V. A. Dubovitskii in the Institute of Chemical Physics in Chernogolovka, RAS) was used for treatment of kinetic curves of the radical ion decay in the case of short-lived products (TMPD, MeODMA) when the lifetime was comparable to the duration of the laser pulse.

The energy of the level with the charge transfer (ΔG) was determined from literature data on the redox potentials of C_{60} and Am. According to previously published data,[35] $E_{1/2}$/eV (Am/Am$^+$) are the following: TMPD, 0.12; MeODMA, 0.55; MeDMA, 0.71; DEA, 0.76; DMA, 0.81; and TPA, 1.12 relative to the calomel electrode in acetonitrile. $E_{1/2}(C_{60}^{-}/C_{60})$ is equal to −0.42 relative to the calomel electrode in benzonitrile,[23,24] and it is −0.51 [22] in acetonitrile with a correction for the medium. $-\Delta G = E_{1/2}(C_{60}^{-}/C_{60}) - E_{1/2}(Am/Am^{+}) - \Delta'$, where Δ' is the semi-empirical correction for the energy of the Coulomb interaction in RIP, which is accepted as equal to 0.1 eV.[15] The data on ΔG are presented in Tables 1 and 2.

Absorption spectra of donor-acceptor complexes between C_{60} and amines. Fullerene C_{60} forms donor-acceptor complexes with amines in solution. The formation of the com-

Table 2. Lifetimes of RIP and corresponding energy parameters

Amine	ΔG /eV	λ /eV	λ_0 /eV	λ_i /eV	λ_i' /eV	V /cm^{-1}	V' /cm^{-1}	τ /ps
TMPD	0.73	0.975	0.414	0.561	0.371	654	39	3±2
MeODMA	1.16	0.872	0.652	0.22	0.291	715	43	11±5
MeDMA	1.32	0.877	0.572	0.315	0.271	667	40	21±7
DEA	1.37	0.775	0.488	0.287	0.282	667	40	56±10
DMA	1.42	0.886	0.554	0.332	0.287	665	40	39±7
TPA	1.73	0.571	0.298	0.273	0.320	569	34	1180±100

Notes: ΔG is the values of the reaction driving force; $\lambda = \lambda_0 + \lambda_i$ is the total reorganization energy (determined from Eq. (8)); λ_i and λ_0 are internal and external reorganization energies (determined by the combined solution of Eqs. (8) and (11)); λ_i' is the internal reorganization energies (found from modelling of the shape of the charge-transfer band); V is the parameters of the electron-electron interaction (determined according to Eq. (12)); V' is the parameters of the electron-electron interaction used in the calculation of k_{ET} for Fig. 8; τ is the experimentally determined lifetimes of RIPs.

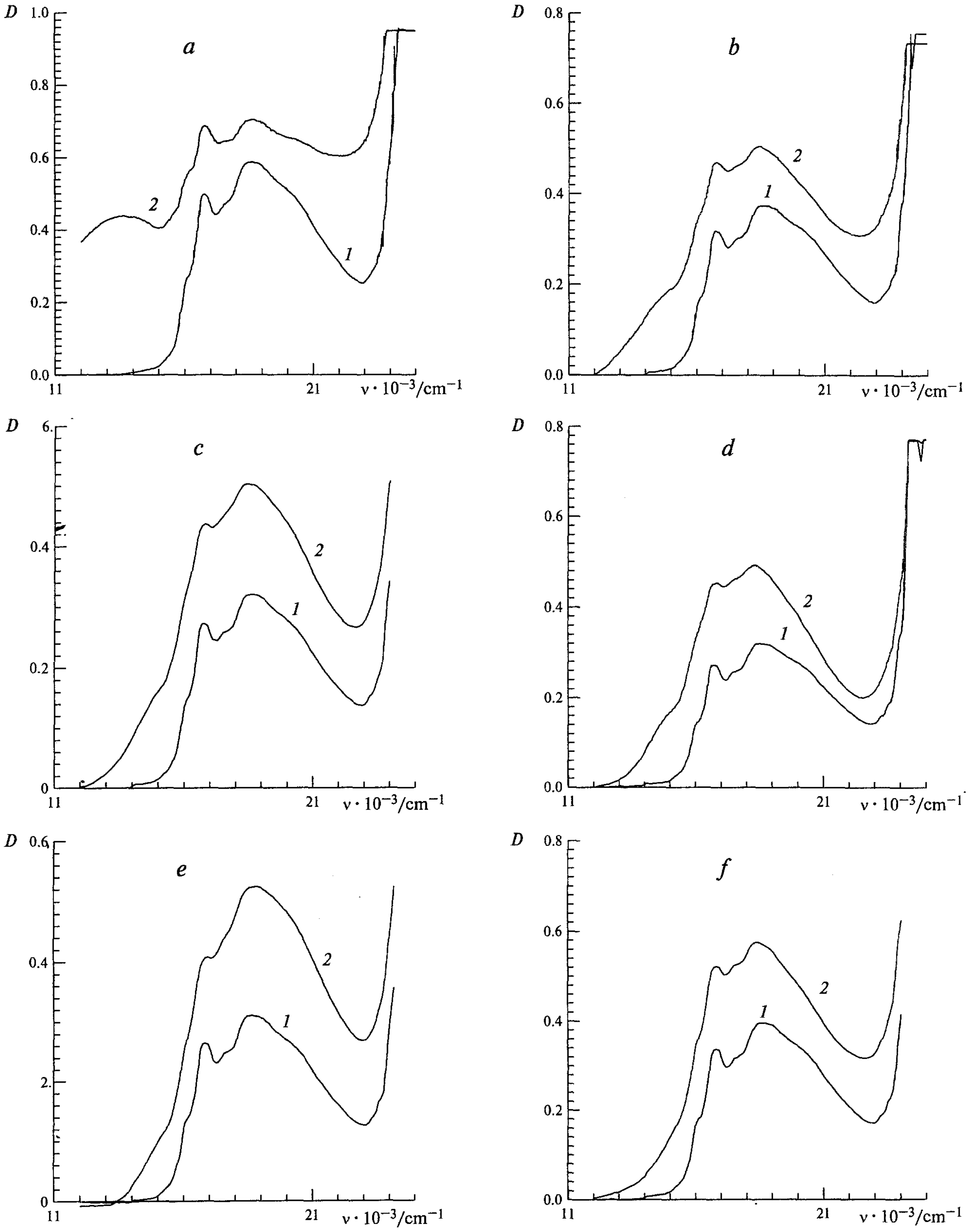

Fig. 1. Absorption spectra of chlorobenzene solutions of C_{60}: *a*, C_{60}/TMPD; *b*, C_{60}/MeODMA; *c*, C_{60}/MeDMA; *d*, C_{60}/DEA; *e*, C_{60}/DMA; *f*, C_{60}/TPA; *1*, with no amine added, *2*, with amine added. System: TMPD—[C_{60}] = 659 μ*M*, [TMPD] = 1.0 *M*; MeODMA—[C_{60}] = 483 μ*M*, [MeODMA] = 1.4 *M*; MeDMA—[C_{60}] = 355 μ*M*, [MeDMA] = 2.0 *M*; DEA—[C_{60}] = 359 μ*M*, [DEA] = 2.1 *M*; DMA—[C_{60}] = 359 μ*M*, [DMA] = 2.3 *M*; TPA—[C_{60}] = 445 μ*M*, [TPA] = 1.2 *M*.

plexes manifests itself as characteristic changes in the absorption in the long-wave region of the optical spectrum (Fig. 1). A new absorption band in the long-wave spectral range or a distinctly pronounced long-wave shoulder appear in the case of amines with the most pronounced electron-donating properties, such as TMPD and MeODMA. For amines with higher oxidation potentials (MeDMA, DEA, DMA, and TPA), the formation of a CTC appears as a change in the shape of the long-wave absorption band of C_{60} and an increase in the optical density when amine is dissolved. The values of the equilibrium constants of the CTC formation and extinction coefficients ϵ were determined from the dependence of the optical density of the solution on the amine concentration in the region of the charge-transfer band. The experimental dependence of the optical density of the solution on the amine concentration is linear in the Benesi—Hildebrand coordinates (Fig. 2), which indicates the presence for the most part of complexes of 1 : 1 composition. Data on the values of equilibrium constants K and extinction coefficients are presented in Table 1. As can be seen from the spectra presented in Fig. 1, the charge-transfer bands and the long-wave absorption band of C_{60} overlap to a considerable extent. The charge-transfer band is significant for the further analysis. Therefore, the absorption spectrum of C_{60}, which was unbound in the complex, was extracted from the total absorption spectrum of the solution $D(\nu)$, in accordance with Eqs. (1) and (2).

$$\frac{[\mathrm{CTC}]}{[\mathrm{C_{60}}][\mathrm{Am}]} = K, \tag{1}$$

$$D(\nu) = \epsilon_{\mathrm{C_{60}}}(\nu)[\mathrm{C_{60}}] + \epsilon_{\mathrm{CTC}}(\nu)[\mathrm{CTC}]. \tag{2}$$

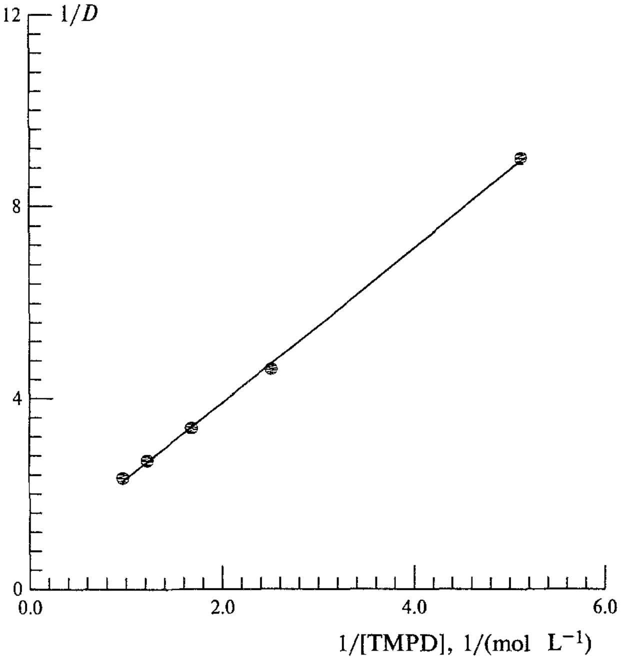

Fig. 2. Dependence of the reverse optical density of a solution of C_{60} with TMPD at 14000 cm^{-1} on the reverse amine concentration; $[C_{60}]$ = 659 μ*M*.

The absorption spectra of a CTC isolated according to Eqs. (1) and (2) are presented in Fig. 3. The data on a maximum of the charge-transfer band and its half-width are presented in Table 1.

The formation of a CTC between C_{60} and amines has previously been reported.[28] The equilibrium constants of the formation of the complexes with DMA[27] and TPA[28] in benzene are approximately an order of magnitude lower than those in chlorobenzene. This difference in the equilibrium constants of the complexes is not surprising on going from the nonpolar medium to the low-polar medium, as it takes place in the case of benzene and chlorobenzene.[36]

Pulse photolysis. It has previously been established[34] in studying the absorption spectra of photoexcited C_{60} in solutions in the absence of amines by picosecond photolysis that the differential S_1—S_x absorption spectrum has a broad absorption band at 450 to 800 nm without characteristic maxima and an absorption band with a pronounced maximum at ~940 nm. The time of the intersystem transition is equal to 1100 to 1200 ps. The absorption of the T_1—T_x transition with a maximum at 750 nm increases in parallel with a decrease in the absorption caused by the S_1—S_x transition.

The addition of amines to a solution of C_{60} results in drastic changes in the intermediate absorption spectra, and the character of the decay of the optical density of the solution also changes compared to a pure solution of C_{60}. These changes can be briefly summarized as follows (the system with TPA exhibits several substantial peculiarities compared to the systems with the other amines studied):

(1) an increase in the amine concentration (from 0.3 to 0.75 mol L^{-1}) results in the acceleration of a decrease in the S_1—S_x absorption of C_{60} (940 nm) and decrease in the intensity of the T_1—T_x transition (750 nm). The kinetic curves of the optical density and intermediate absorption spectra are more complicated compared to those for the experiments with zero and extremely high concentrations of amine (more than 1 mol L^{-1}). More complicated characteristics of spectra are caused by the appearance of the absorption of the products of a radical ion nature at such concentrations of amine, along with the S_1—S_x and T_1—T_x absorption;

(2) when the concentration of amine is >1.2 mol L^{-1}, intermediate absorption spectra become considerably simpler and contain the characteristic band with a maximum at 1070 nm, which is inherent of all the studied systems with amines, and shorter-wave bands, whose positions depend on the nature of the amine (Fig. 4). The band with a maximum at 1070 nm coincides with the absorption band of the C_{60}^- radical anion, and the maxima of the short-wave bands correspond to the absorption of the radical cation of amine. The characteristic T_1—T_x absorption band of C_{60} (750 nm) disappears at high concentrations of amine. The exception is the system with TPA, for which the T1—Tx absorption is also observed at high concentrations of TPA (Fig. 5);

(3) the rate of the decrease in the optical density at the absorption maximum of C_{60} (1070 nm) coincides with the rate of the decrease in the absorption maximum of the amine radical cation. It is determined by the multiexponential decay law. The typical kinetic curves for the decay of radical ion pairs are presented in Fig. 5. The data on the lifetimes of these pairs are listed in Table 2;

(4) the formation of RIPs at high concentrations of amine occurs in a time that is considerably shorter than the duration of the laser pulse and is ≤2 ps. This value agrees with the data of Ref. 26, where the time of the RIP formation for the CTC between C_{60} and DMA was measured in benzene and was approximately equal to 1 ps.

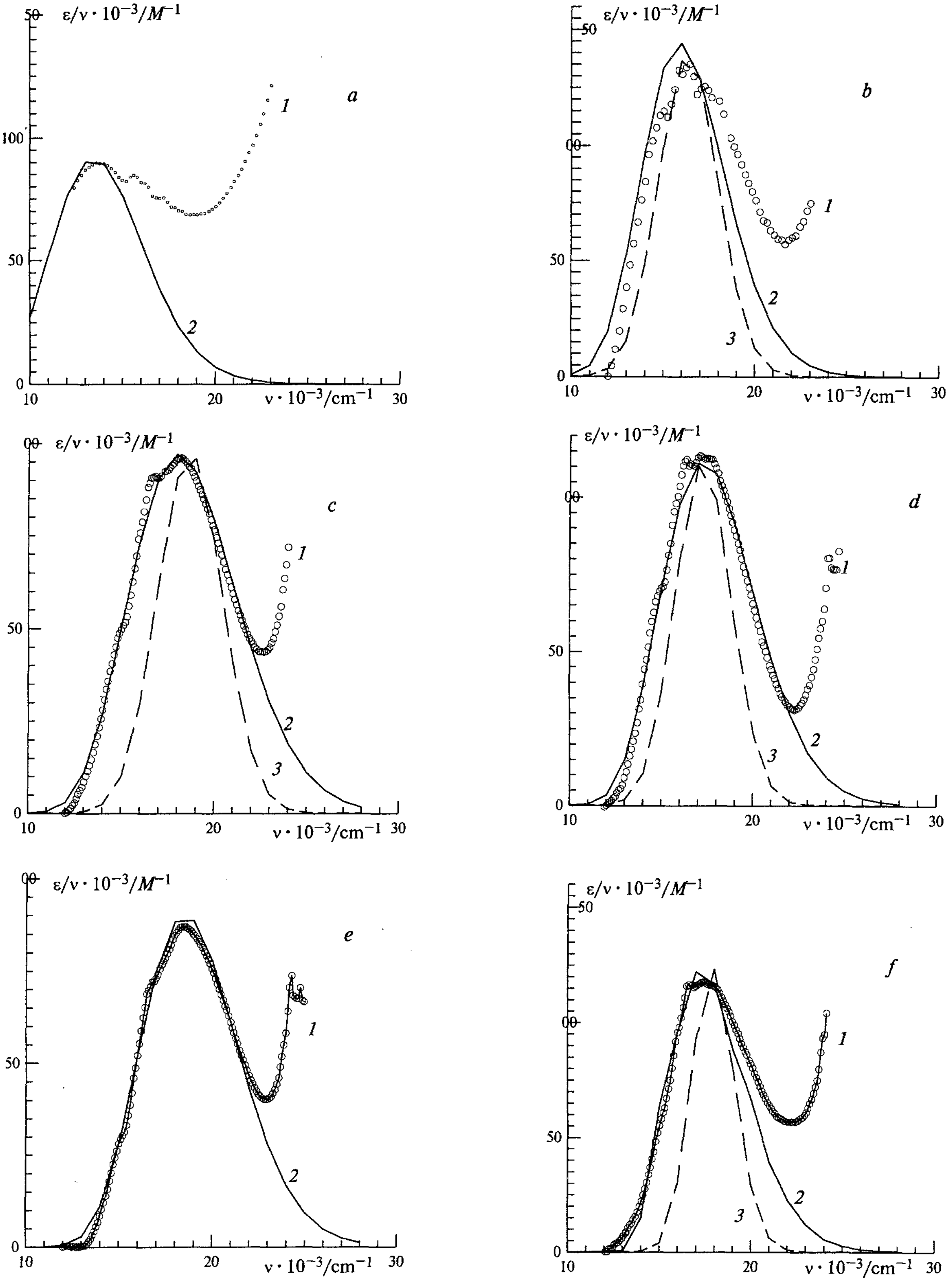

Fig. 3. Isolated charge-transfer bands of C_{60} with amines: *a*, C_{60}/TMPD; *b*, C_{60}/MeODMA; *c*, C_{60}/MeDMA; *d*, C_{60}/DEA; *e*, C_{60}/DMA; *f*, C_{60}/TPA. The bands are presented according to Eq. (3). The parameters λ_i' are summarized in Table 2. *1*, experimental data; *2*, calculated shape of the band at a vibration frequency of 1500 cm^{-1}; *3*, calculated shape of the band at a vibration frequency of 400 cm^{-1}.

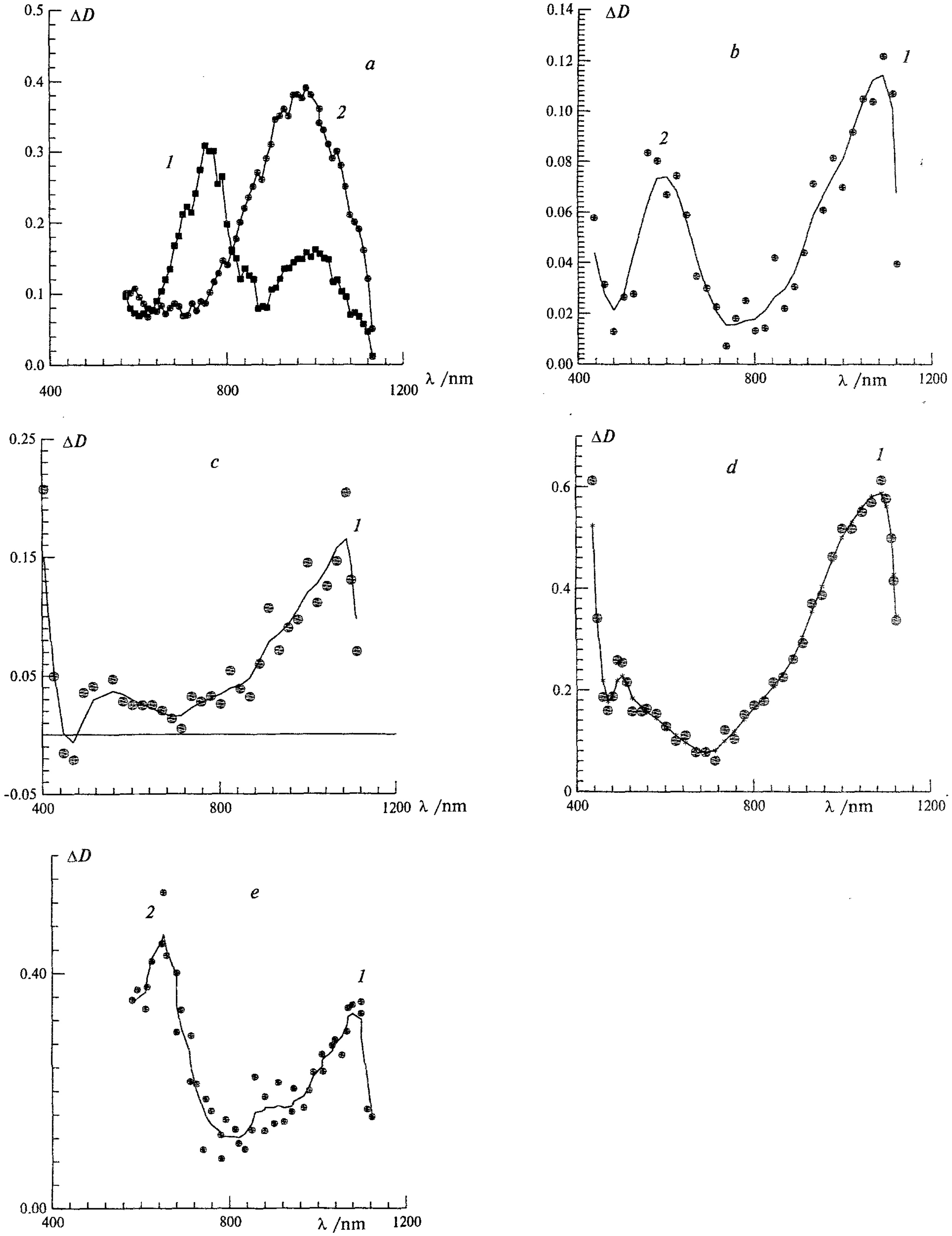

Fig. 4. Picosecond intermediate absorption spectra of solutions of C_{60} in the presence and absence of amines. $[C_{60}] = 6 \cdot 10^{-4}$ *M*; [TMPD] = 1.7 *M*; [MeODMA] = 1.6 *M*; [MeDMA] = 1.5 *M*; [TPA] = 2.0 *M*. In the systems with amines, the spectra were obtained with a zero time delay. *a*, C_{60}; *b*, C_{60}/TMPD: *1*, C_{60}^{-}, *2*, $TMPD^{+}$; *c*, C_{60}/MeODMA: *1*, C_{60}^{-}; *d*, C_{60}/MeDMA: *1*, C_{60}^{-}; *e*, C_{60}/TPA: *1*, C_{60}^{-}; *2*, TPA^{+}.

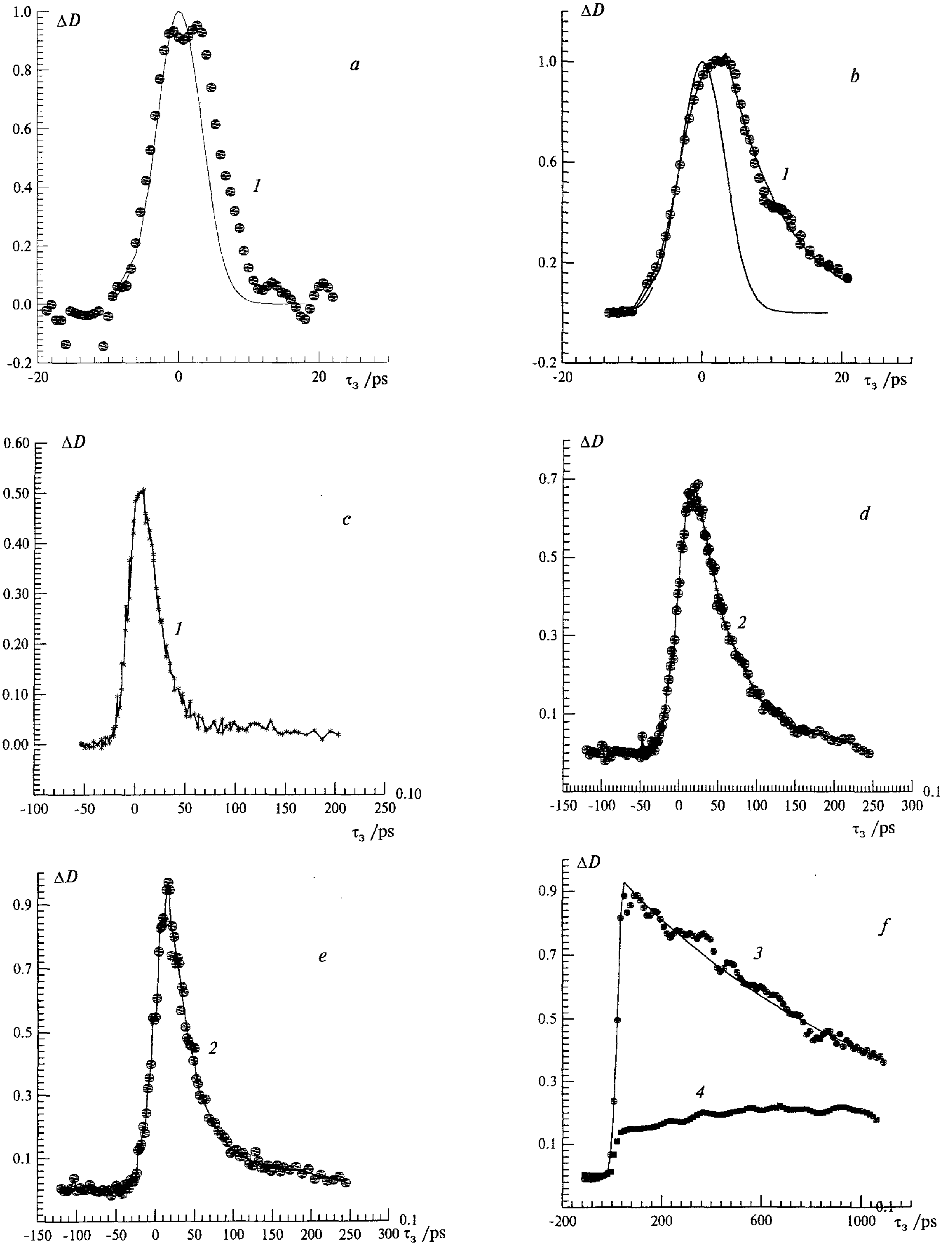

Fig. 5. Kinetic curves of the induced optical density in picosecond laser photolysis. In the systems with TMPD and MeODMA, the spread function of the laser pulse is shown by solid lines. The wavelength of the detection of the decay of C_{60}^{-1}: *1*, 1053 nm; *2*, 1060 nm; *3*, 650 nm; *4*, 750 nm. *a*, C_{60}/TMPD; *b*, C_{60}/MeODMA; *c*, C_{60}/MeDMA; *d*, C_{60}/DEA; *e*, C_{60}/DMA; *f*, C_{60}/TPA.

Results and Discussion

Both unbound C_{60} molecules and donor-acceptor charge-transfer complexes are excited in solutions of C_{60} and amine. The formation of the products of radical ion nature is caused by dynamic quenching of the S_1 state of C_{60}, excitation of the CTC of C_{60} to the charge-transfer state, and quenching of the S_1 state of C_{60} by the amine molecule in the statistic pair (the amine molecule is in the first solvate shell of C_{60} in the statistic nature of quenching[36]). It is assumed that a solvate-separated RIP is formed in the dynamic quenching, while a contact RIP is formed in the last two cases. In the further discussion we will not distinguish between RIPs formed by the excitement of the CTC with the charge transfer and RIPs formed in statistic pairs, unifying them by the notion of the contact RIP. Thus, the formation of RIP can be presented as follows:

Scheme 1

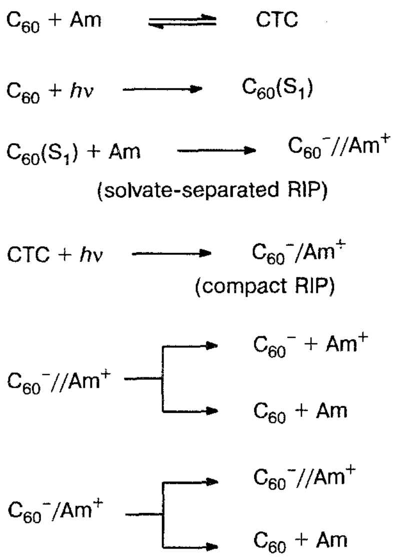

The contact C_{60}^{-}/Am^{+} pairs are mainly formed when the concentrations of amine are higher than 1 to 1.2 mol L^{-1}, and the channel of dynamic quenching does not predominate. The back electron transfer between the C_{60}^{-} radical anion and the amine radical cation, which are transformed to the ground singlet state, is *a fortiori* the main channel of decay of RIPs in the systems with TMPD, MeODMA, MeDMA, DEA, and DMA. The energy levels of the charge-transfer states of these CTCs are substantially lower than the excited levels of C_{60} (the lowest triplet level of C_{60} lies at 1.56 eV [37]) and amine (see Table 2). In the system with TPA, the level with the charge transfer is close to the triplet (T_1) and singlet (S_1) levels of C_{60} (see Table 2), and therefore, the charge recombination of RIPs to the triplet $C_{60}(T_1)$ or singlet $C_{60}(S_1)$ states cannot in principle be ruled out. The observed rate constant of charge recombination in the RIP with TPA is the upper limit for the rate constant of charge separation to the ground singlet state. However, additional study of the dynamics of the triplet RIPs of C_{60} with TPA shows that the value of the rate constant of the decay of the RIP with TPA is hardly related to the charge recombination to the $C_{60}(T_1)$ state.

According to the modern views,[9] the shape of the charge-transfer band in absorption and fluorescence spectra is determined by Eqs. (3) and (4), respectively, in the single-mode quantum approximation:

$$\varepsilon(\nu)/\nu = C_a h \sum \frac{e^{-S} S^n \exp[-(n\hbar\omega + \Delta G + \lambda_0 - h\nu)^2 / 4\lambda_0 k_B T]}{n!(4\pi\lambda_0 k_B T)^{0.5}}, \quad (3)$$

$$f(\nu)/\nu^3 = C_f h \sum \frac{e^{-S} S^n \exp[-(n\hbar\omega + \Delta G + \lambda_0 + h\nu)^2 / 4\lambda_0 k_B T]}{n!(4\pi\lambda_0 k_B T)^{0.5}}, \quad (4)$$

where C_a and C_f are constants that are proportional to the square dipole moment of the transition in the charge-transfer band; $S = \lambda_{in}/\hbar\omega$ is the parameter of electron-vibration interaction, and $\hbar\omega$ is the quantum of the vibration energy of the oscillator active in the electron transfer process.

The nonradiative relaxation of the charge-transfer state in the CTC or, in other words, the electron transfer in the contact RIP is determined by the rate constant according to the following expression[1]:

$$k_{ET} = \frac{2\pi V^2}{\hbar\sqrt{4\pi\lambda_0 k_B T}} \times \sum \frac{e^{-S} S^n \exp[-(n\hbar\omega + \lambda_0 - \Delta G)^2 / 4\lambda_0 k_B T]}{n!(1 + H_n)}, \quad (5)$$

where the factor of nonadiabatic character (H_n) is determined by the expression[1]:

$$H_n = \frac{4\pi V^2 \tau_L}{\hbar\lambda_0} \frac{S^n}{n!} e^{-S}, \quad (6)$$

In the case when the value of the electron-electron interaction V is low and $H_n << 1$, Eq. (5) is transformed into an expression for the rate constant of the nonadiabatic electron transfer[1]:

$$k_{ET} = \frac{2\pi V^2}{\hbar\sqrt{4\pi\lambda_0 k_B T}} \times \sum e^{-S} \frac{S^n}{n!} \exp[-\frac{(n\hbar\omega + \lambda_0 - \Delta G)^2}{(4\lambda_0 k_B T)}]. \quad (7)$$

Since Eqs. (3) and (4) for the optical transitions and Eq. (5) for the nonradiative transition describe the relaxation of the same charge-transfer state, it can be expected that the values of the parameters of the reorganization energy λ_0 and λ_{in} and frequency ω are equal.*

In addition, the following several correlations between the maxima of absorption and fluorescence bands, ΔG, and the reorganization energy should be fulfilled:

$$h\nu_{max} = \Delta G + \lambda_0 + \lambda_i, \qquad (8)$$

$$h\nu^a_{max} - h\nu^f_{max} = 2(\lambda_0 + \lambda_i), \qquad (9)$$

$$\frac{h(\nu^a_{max} + \nu^f_{max})}{2} = \Delta G. \qquad (10)$$

However, the intensity of the fluorescence of CTC between C_{60} and amines turned out to be so low that we failed to detect it. Therefore, the position of the maximum of the absorption band and the ΔG value obtained from the electrochemical data were used in practice for estimating the reorganization energy. In addition, it is useful to take into account the fact that the half-width of the charge-transfer band is approximately related to the reorganization energy according to the expression:

$$W_{1/2} = 2\sqrt{[2\lambda_0 k_B T + \lambda_i \hbar\omega \coth(\frac{\hbar\omega}{2k_B T})](2\ln 2)} \quad , \qquad (11)$$

The values $\lambda = \lambda_0 + \lambda_i$ presented in Table 2 are determined from Eq. (8). Equations (8) and (11) contain two unknown values λ_0 and λ_{in} and an indefinite value of the frequency ω. When it is assumed (as commonly accepted in the literature[11–19]) that the frequency $\hbar\omega$ = 1500 cm^{-1} (corresponding to the frequency of the C=C vibrations), it is easy to calculate the values of λ_0 and λ_{in} from Eqs. (8) and (11). These data are also presented in Table 2. It is noteworthy that the values of the reorganization energy can also be determined from Eq. (3), modelling the shape of the absorption band by the variation of C_a, λ_0, λ_i, and ω. The values of $\hbar\omega$ = 1500 cm^{-1}, ΔG, and λ presented in Table 2 were used to make this fitting more definite. Thus, only the parameters C_a and λ_i were varied using the condition $\lambda = \lambda_0 + \lambda_i$ (the consequence of Eq. (8)). The obtained values of λ_i' are also presented in Table 2. The reorganization energy changes drastically in the series of the complexes studied, which is the reason for a relatively poor correlation between ΔG and ν_{max} (see Table 2).

When it is assumed that the low-frequency vibrations $\hbar\omega$ = 500 cm^{-1} are active in the electron transfer and substantial in the formation of the charge-transfer band, it turns out that the system of two Eqs. (8) and (10) has no formal solutions for positive λ values. The modelling of the shape of the band on the assumption of the low frequency results in the contradiction between the theory and experiment: the calculated band is considerably narrower (its half-width is smaller). Comparison of the experimentally observed shapes of the bands with the calculated shapes is presented in Fig. 3. An assumption of a low value of the reorganization energy $\lambda_i < 0.1$ eV and ω_i = 1500 cm^{-1} results in a similar contradiction between the theory and experiment.

To determine the parameter k_{ET}, the value of the parameter V should also be known. According to Mulliken's theory about CTC spectra, the extinction coefficient and V are related by the simple expression:

$$\epsilon_{max} = \frac{707.6V^2\alpha^2R^2}{h\nu_{max}\sqrt{\lambda_0 k_B T}}, \qquad (12)$$

where α is a coefficient which is close to 1; R is the distance between the donor and acceptor molecules, which is equal to 9 Å.

The V values obtained from Eq. (12) are presented in Table 2.** As can be seen from Table 2, these values range from 570 to 720 cm^{-1}. The V values obtained are typical of other systems of CTCs. Similar V values are also observed in other cases.[13,17–19]

As can be seen from the data in Table 2, the rate constant of the relaxation of the charge-transfer state (the decay of the contact RIP) k_{ET} decreases ~1000 times when ΔG changes by 1 eV in the series of amines studied. From the viewpoint of checking the theoretical concepts about k_{ET} and the relation of the parameters determining the shape of the charge transfer band and k_{ET}, the following questions are of interest: how does k_{ET} depend on ΔG, according to Eqs. (5) or (7), or is this dependence exponential ($k_{ET} = A \cdot \exp(-\beta|\Delta G|)$), as is assumed in Refs. 3 and 16; do experimental and calculated values of k_{ET} differ when starting from the data on V and $\lambda_{0,i}$ for the charge-transfer band?

The analysis of the dependence of k_{ET} on ΔG can be performed starting from different assumptions. The approach which is the most common in the literature is based on the analysis of the dependence of the rate constant on the driving force ΔG in the homological series of reactions on the assumption that all of these reactions are characterized by similar values of the parameters V, $\lambda_{0,i}$, and ω.[10,11,15] We prefer to use a nonadiabatic model (Eq. (7))[10,11,15,17–19] for the analysis. The V and $\lambda_{0,i}$ parameters are determined from the

---

* For a more rigorous treatment, the reorganization energies of the absorption λ_{in}(abs) and fluorescence λ_{in} (fluor) bands must be considered to differ. The parameters determined from the fluorescence band are more suitable for calculation of the rate constant of the electron transfer. Nevertheless, this difference can be neglected, because the rule of mirror symmetry for the absorption and fluorescence bands is fulfilled experimentally in the majority of cases.

** The V value can also be determined from the C_a values obtained previously. The same physical prerequisite is used as in the case of Eq. (12): the dipole moment of the transition is proportional to V and R.

dependence of k_{ET} on ΔG by fitting the theoretical curve to the experiment. When V and $\lambda_{0,i}$ are determined by this method, it is seen that satisfactory agreement of the theoretical curve with the experimental dependence is achieved at V = 50 cm^{-1}, λ_0 = 0.53 eV, and λ_{in} = 0.3 eV (Fig. 6). It follows from this analysis that the V values determined from the spectral and kinetic data differ significantly, which seems to be related to the fact that the values of the parameter H_n in the case of chlorobenzene can be much higher than 1 at V = 660 cm^{-1}. For example, for chlorobenzene τ_L = 5.7 ps when starting from the value τ_D = 12.5 ps [39] (ε_s = 5.62 and ε_0 = 2.58 [39]). Figure 6 presents the dependence of k_{ET} on ΔG according to Eq. (5) and using the average parameters from Table 2 in the series of amines: V = 656 cm^{-1}, λ_{in} = 0.3 eV, and λ_0 = 0.53 eV. As can be seen from Fig. 7, the limiting value of k_{ET} calculated by Eq. (5) is close to $10^{11.5}$ s^{-1} and nearly coincides with the experimentally measured limiting value of k_{ET}. However, the shape of the dependence for the vibration frequency $\hbar\omega$ = 1500 cm^{-1} is reproduced unsatisfactorily. In the range of high values of ΔG, the calculated values of the constants exceed the experimental values by more than two orders of magnitude. At the same time, satisfactory agreement between the calculated and experimental curves can be achieved on the assumption of the low vibration frequency $\hbar\omega$ = 400 cm^{-1}.

The following approach seems more valid: for each contact RIP its inherent parameters $\lambda_{0,i}$ and V are assumed, found from the optical spectra (see Table 2), and the k_{ET} value is calculated according to the model chosen. The dependences of k_{ET} on ΔG calculated by Eq. (7) using the values of the reorganization energy for each RIP from Table 2 are presented in Fig. 8. Decreased values of V' are chosen, but the ratio of the V' values for different amines is the same as that between the V values obtained from the spectral data. It is seen from Fig. 8 that agreement between calculation and experiment can thus be achieved, but the V values should be *a fortiori* decreased. The curves calculated on the basis of Eq. (5), using all necessary parameters obtained from the spectral data, are presented in Fig. 9. As can be seen from Fig. 9, the calculated rate constants coincide within an order of magnitude with the experimentally measured rate constants on the assumption of a low vibration frequency $\hbar\omega$ = 500 cm^{-1}. In the case of high-frequency vibrations $\hbar\omega$ = 1500 cm^{-1}, a weaker dependence of the rate constant on ΔG compared to the experimentally observed dependence can be theoretically predicted. The results of the preceding analysis can be summarized as follows:

— the dependence of k_{ET} on ΔG can be formally described on the basis of the nonadiabatic model (7), starting from the values of the reorganization energies obtained from the spectra of the CTC, but the chosen V values should be decreased, which is physically unjustified;

— the same dependence based on model (5) taking

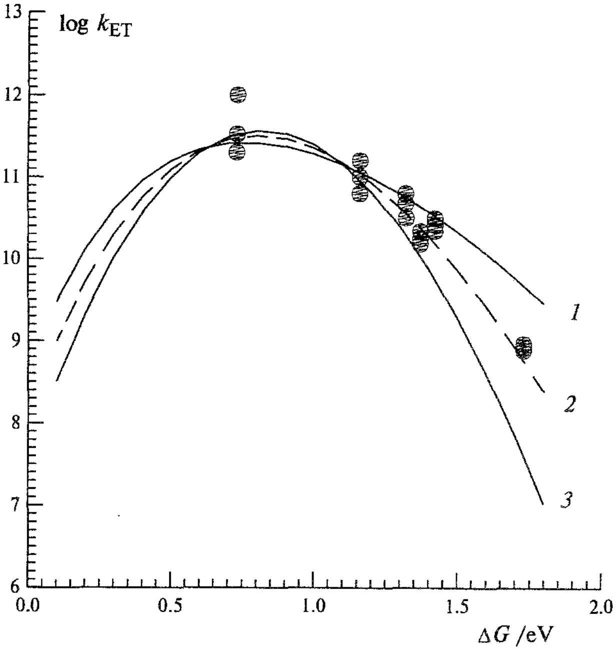

Fig. 6. Dependence of the rate constant of the decay of an RIP on ΔG. Experimental data are shown by points; lines indicate calculation by the nonadiabatic model (7) at the following values of the parameters for all three curves: V = 50 cm^{-1}, λ_i = 0.30 eV, λ_0 = 0.527 eV. Vibration frequency (cm^{-1}): *1*, 1500; *2*, 750; *3*, 400.

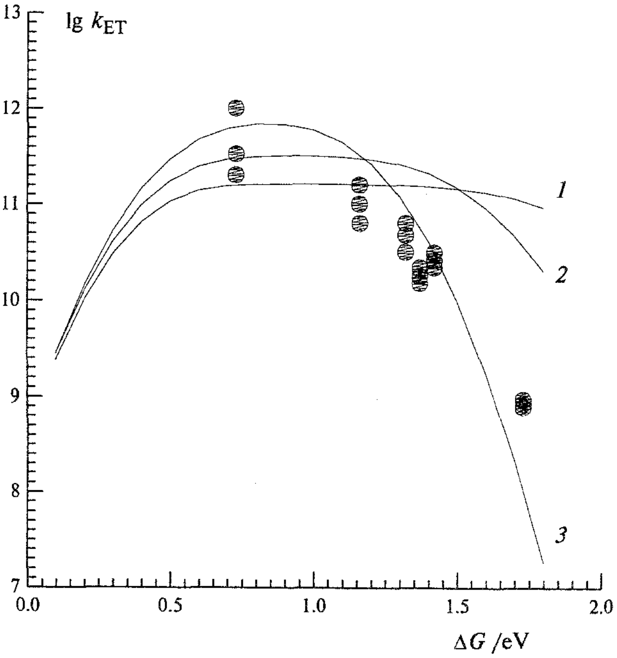

Fig. 7. Dependence of the rate constant of the decay of an RIP on ΔG. Experimental data are shown by points; lines indicate calculation by the nonadiabatic model (5) at the following values of the parameters for all three curves: V = 565 cm^{-1}, λ_i = 0.30 eV, λ_0 = 0.527 eV. Vibration frequency (cm^{-1}): *1*, 1500 cm^{-1}; *2*, 750 cm^{-1}; *3*, 400 cm^{-1}.

account of the adiabatic correction can be described only on the assumption of the low-frequency vibrations close to 500 cm^{-1};

— the shape of the charge-transfer band is poorly described on the assumption of the low-frequency vibrations (the calculation gives *a fortiori* decreased values of the half-width of the band), and a significantly better agreement is achieved on the assumption of the high-frequency vibrations.

The models of the band shape and rate constant considered are based on the artificial but commonly accepted single-mode approximation. It is evident that more than one vibration is active in the electron transfer. This is confirmed by the experimental results on studying the Raman resonance spectra near the charge-transfer band of the CTC between tetracyanoethylene and hexamethylbenzene.[20] It has been shown that three types of vibrations are active in the electron transfer due to the optical transition in the charge-transfer band: high-frequency (3500 cm^{-1}), medium-frequency (1551 cm^{-1}), and low-frequency (165 cm^{-1}) vibrations (the latter correspond to intramolecular vibrations of a donor and acceptor). The contribution of the reorganization energy related to the low-frequency vibrations to the value of the total internal reorganization energy is about 40 %.[20] The vibrations of the spherical framework of the cluster with frequencies of ~500 cm^{-1} are typical of the C_{60} system.[40] It is quite probable that these vibrations are active in the process of back electron transfer in the contact RIPs with C_{60}. Anyway, we should admit that presently there is no physically justified method for choosing the frequency of active vibrations for the single-mode approximation. The parameters of the reorganization energies $\lambda_{0,i}$ and V agree semi-quantitatively with the spectral and kinetic data in terms of the adiabatic model and single-mode approximation (5), but with different frequencies of the active vibrations $\hbar\omega$ they agree with the optical density (1500 cm^{-1}) in Eq. (3) and with the electron transfer (~500 cm^{-1}) in Eq. (5). In addition to this, experimental results on the electron transfer kinetics in contact RIPs can be described on the basis of the single-mode non-adiabatic model (7) on the assumption of the same vibration frequencies $\hbar\omega$ for the optical transition and electron transfer, but the V values for these two cases should differ by an order of magnitude.

As for the empirical dependence $k_{ET} = A \cdot \exp(-\beta|\Delta G|)$, the β parameter in the series of RIPs between C_{60} and amines is equal to 5.95 1/eV. This value is 3 to 4 times higher than β for the series of CTCs of aromatic hydrocarbons with tetracyanoquinodimethane and tetracyanoethylene in acetonitrile[16] and ~2 times higher for the series of CTCs of aromatic hydrocarbons with methyl viologen in the micelles of NaLS.[12,13] However, it should be mentioned that the exponential dependence $k_{ET} = A \cdot \exp(-\beta|\Delta G|)$ is fulfilled in the rough approximation (see Fig. 6).

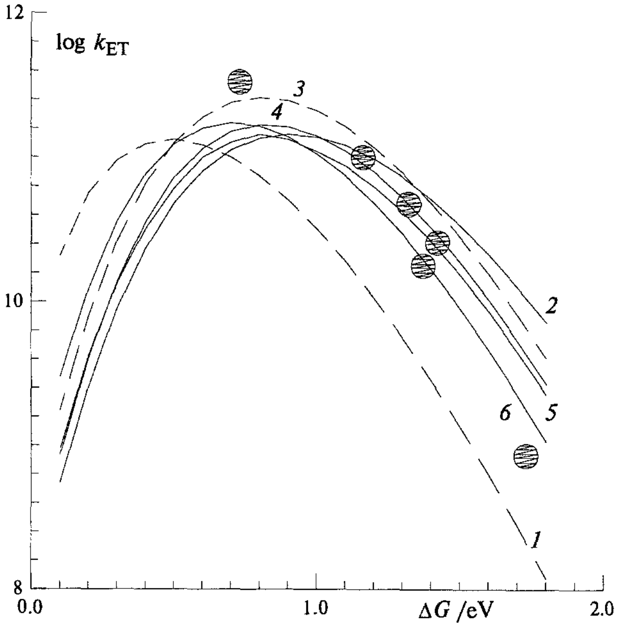

Fig. 8. Dependence of the rate constant of the decay of an RIP on ΔG. Experimental data (average values) are indicated by points; a calculation by the nonadiabatic model is shown by lines, frequency 1500 cm^{-1}: *1*, TPA; *2*, TMPD; *3*, MeODMA; *4*, MeDMA; *5*, DMA; *6*, DEA (the values of V' and λ_i' are summarized in Table 2 for each amine).

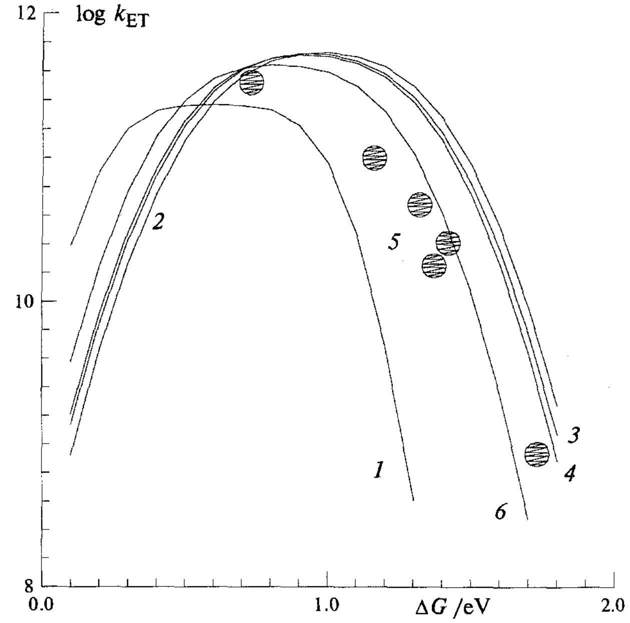

Fig. 9. Dependence of the rate constant of the decay of an RIP on ΔG. Experimental data (average values) are indicated by points; a calculation by the nonadiabatic model is shown by lines, frequency 400 cm^{-1}: *1*, TPA; *2*, TMPD; *3*, MeODMA; *4*, MeDMA; *5*, DMA; *6*, DEA (the values of V' and λ_i' are summarized in Table 2 for each amine).

The authors are grateful to D. V. Khudyakov and I. V. Rubtsov for help in experiments and to A. S. Lobach for the C_{60} supplied.

The work was financially supported by the Russian Foundation for Basic Research (Projects No. 93-03-05254 and 93-03-0217).

References

1. J. Jortner and M. Bixon, *J. Chem. Phys.*, 1988, **88**, 167.
2. R. R. Dogonadze and A. M. Kuznetsov, *Kinetika geterogennykh khimicheskikh reaktsii v rastvorakh* [*Kinetics of Heterogeneous Chemical Reactions in Solutions*], VINITI, Moscow, 1978, **5**, 223 (in Russian).
3. T. Asahi and N. Mataga, *J. Phys. Chem.*, 1989, **93**, 6575.
4. N. Mataga and M. Ottolenghi, in *Molecular Association*, Ed. R. Foster, Academic, New York, 1979, **2**, 1.
5. R. A. Marcus and N. Sutin, *Biochim. Biophys. Acta*, 1985, **811**, 265.
6. U. Sumi and R. A. Marcus, *J. Chem. Phys.*, 1986, **84**, 411.
7. M. Sparpaglione and S. Mucamel, *J. Chem. Phys.*, 1988, **88**, 3663.
8. M. Sparpaglione and S. Mucamel, *J. Chem. Phys.*, 1988, **88**, 4300.
9. R. A. Marcus, *J. Phys. Chem.*, 1989, **93**, 3028.
10. I. R. Gould, D. Ege, J. E. Moser, and S. Farid, *J. Am. Chem. Soc.*, 1990, **112**, 4290.
11. I. R. Gould, R. H. Yong, R. E. Moody, and S. Farid, *J. Phys. Chem.*, 1991, **95**, 2068.
12. S. M. Hubig, *J. Phys. Chem.*, 1992, **96**, 2903.
13. V. A. Nadtochenko, N. N. Denisov, V. Gul'binas, V. Butvilas, and A. Urbas, *Zh. Fiz. Khim.*, 1993, **67**, 2469 [*Russ. J. Phys. Chem.*, 1993, **67** (Engl. Transl.)].
14. S. L. Logunov and M. A. J. Rodgers, *J. Phys. Chem.*, 1992, **96**, 8697.
15. P. P. Levin, P. F. Pluzhnikov, and V. A. Kuzmin, *Chem. Phys.*, 1989, **137**, 331.
16. T. Asahi and N. Mataga, *J. Phys. Chem.*, 1991, **95**, 1956.
17. J. R. Gould, D. Ege, J. S. Moser, and S. Farid, *J. Am. Chem. Soc.*, 1990, **112**, 4290.
18. J. R. Gould and S. Farid, *J. Phys. Chem.*, 1993, **97**, 1306.
19. J. R. Gould, D. Noukakis, L. Gomez-Jahn, J. L. Goodman, and S. Farid, *J. Am. Chem. Soc.*, 1993, **115**, 4405.
20. F. Markel, S. Nancy, N. S. Ferris, J. R. Gould, and A. B. Myers, *J. Am. Chem. Soc.*, 1992, **114**, 6208.
21. K. W. Penfield, J. R. Miller, M. N. Paddon-Row, E. Cotsaris, A. M. Oliver, and N. S. Hush, *J. Am. Chem. Soc.*, 1987, **109**, 5061.
22. J. W. Arbogast, C. S. Foote, and M. Kao, *J. Am. Chem. Soc.*, 1992, **114**, 2277.
23. D. Dubois, K. M. Kadish, S. Flagan, R. E. Haufler, L. P. F. Chobante, and L. J. Wilson, *J. Am. Chem. Soc.*, 1991, **113**, 4364.
24. D. Dubois, K. M. Kadish, S. Flagan, and L. J. Wilson, *J. Am. Chem. Soc.*, 1991, **113**, 7773.
25. R. J. Sension, C. M. Phillips, A. Z. Szarka, W. J. Romanow, A. R. McGhie, McCauley, Jr., A. B. Smith, and R. M. Hochstrasser, *J. Phys. Chem.*, 1991, **95**, 6075.
26. R. J. Sension, A. Z. Szanka, G. R. Smith, and R. M. Hochstrasser, *Chem. Phys. Lett.*, 1991, **185**, 179.
27. D. K. Palit, H. N. Ghosh, H. Paul, A. V. Sapre, J. P. Mittal, R. Seshadri, and C. N. R. Rao, *Chem. Phys. Lett.*, 1992, **198**, 113.
28. Y. Wang, *J. Chem. Phys.*, 1992, **96**, 764.
29. R. Seshadri, C. N. R. Rao, H. Pal, T. Mukherjee, and J. P. Mittal, *Chem. Phys. Lett.*, 1993, **205**, 395.
30. L. Biczok, H. Linschitz, and R. I. Walter, *Chem. Phys. Lett.*, 1992, **195**, 339.
31. P. V. Kamat, *J. Am. Chem. Soc.*, 1991, **113**, 9705.
32. W. Kratschhmer, L. D. Lamb, K. Fostiropoulos, and D. R. Huffman, *Nature*, 1990, **347**, 354.
33. H. A. Benesi and J. H. Hildebrand, *J. Am. Chem. Soc.*, 1949, **71**, 2703.
34. V. A. Nadtochenko, I. V. Vasil'ev, N. N. Denisov, I. V. Rubtsov, A. S. Lobach, A. P. Moravskii, and A. F. Shestakov, *J. Photochem. Photobiol. A*, 1993, **70**, 153.
35. C. R. Bock, J. A. Conner, T. J. Meyer, D. G. Whitten, B. P. Sullivan, and J. K. Nagle, *J. Am. Chem. Soc.*, 1979, **101**, 4815.
36. R. Foster, *Organic Charge-Transfer Complexes*, Acad. Press, London—New York, 1969, 428.
37. Y. Zeng, L. Biszok, and H. Linschitz, *J. Phys. Chem.*, 1992, **96**, 5237.
38. R. S. Mulliken and W. B. Person, *Molecular Complexes*, Wiley, New York, 1969, 312.
39. Ya. Yu. Akhadov, *Dielektricheskie svoistva binarnykh rastvorov* [*Dielectric Properties of Binary Solutions*], Nauka, Moscow, 1977, 224 (in Russian).
40. D. S. Bethune, G. Meijer, W. C. Tang, H. J. Rosen, W. G. Golden, H. Seki, C. A. Brown, and M. S. deVries, *Chem. Phys. Lett.*, 1991, **179**, 181.

Received September 13, 1994